PHYSICAL REVIEW D **96,** 114017 (2017)

Mass spectra for $qc\bar{q}\bar{c}$, $sc\bar{s}\bar{c}$, $qb\bar{q}\bar{b}$, $sb\bar{s}\bar{b}$ tetraquark states with $J^{PC}=0^{++}$ and 2^{++}

Wei Chen,[1,2] Hua-Xing Chen,[3,*] Xiang Liu,[4,5,†] T. G. Steele,[1,‡] and Shi-Lin Zhu[6,7,8,§]

[1]*School of Physics, Sun Yat-Sen University, Guangzhou 510275, China*
[2]*Department of Physics and Engineering Physics, University of Saskatchewan, Saskatoon, Saskatchewan S7N 5E2, Canada*
[3]*School of Physics and Nuclear Energy Engineering and International Research Center for Nuclei and Particles in the Cosmos, Beihang University, Beijing 100191, China*
[4]*School of Physical Science and Technology, Lanzhou University, Lanzhou 730000, China*
[5]*Research Center for Hadron and CSR Physics, Lanzhou University and Institute of Modern Physics of CAS, Lanzhou 730000, China*
[6]*School of Physics and State Key Laboratory of Nuclear Physics and Technology, Peking University, Beijing 100871, China*
[7]*Collaborative Innovation Center of Quantum Matter, Beijing 100871, China*
[8]*Center of High Energy Physics, Peking University, Beijing 100871, China*

(Received 5 July 2017; published 15 December 2017)

We have studied the mass spectra of the hidden-charm/bottom $qc\bar{q}\bar{c}$, $sc\bar{s}\bar{c}$ and $qb\bar{q}\bar{b}$, $sb\bar{s}\bar{b}$ tetraquark states with $J^{PC}=0^{++}$ and 2^{++} in the framework of QCD sum rules. We construct ten scalar and four tensor interpolating currents in a systematic way and calculate the mass spectra for these tetraquark states. The $X^*(3860)$ may be either an isoscalar tetraquark state or $\chi_{c0}(2P)$. If the $X^*(3860)$ is a tetraquark candidate, our results prefer the 0^{++} option over the 2^{++} one. The $X(4160)$ may be classified as either the scalar or tensor $qc\bar{q}\bar{c}$ tetraquark state, while the $X(3915)$ favors a 0^{++} $qc\bar{q}\bar{c}$ or $sc\bar{s}\bar{c}$ tetraquark assignment over the tensor one. The $X(4350)$ cannot be interpreted as a $sc\bar{s}\,\bar{c}$ tetraquark with either $J^{PC}=0^{++}$ or 2^{++}.

DOI: 10.1103/PhysRevD.96.114017

I. INTRODUCTION

In B factories, the two photon fusion process $\gamma\gamma \to X$ is used to produce C-even charmonium states. To date, the Belle Collaboration has reported three charmnomiumlike states in this process. They are the $Z(3930)$ state in the $\gamma\gamma \to D\bar{D}$ process [1], the $X(3915)$ state in $\gamma\gamma \to \omega J/\psi$ process [2], and the $X(4350)$ state in the $\gamma\gamma \to \phi J/\psi$ process [3]. Since these three states were produced in the $\gamma\gamma$ fusion process, their possible quantum numbers can be either $J^{PC}=0^{++}$ or 2^{++}.

In 2008, Belle analyzed the double charmonium production $e^+e^- \to J/\psi D^{*+}D^{*-}$ process and found a new charmoniumlike structure $X(4160)$ with a significance of 5.1σ [4]. At present, the $D^{*+}D^{*-}$ is the only observed decay mode for the $X(4160)$ state. If $e^+e^- \to J/\psi X(4160)$ is dominant by $e^+e^- \to \gamma^* \to J/\psi X(4160)$, the C parity of $X(4160)$ should be positive. Very recently, Belle performed a full amplitude analysis of the double charmonium production process $e^+e^- \to J/\psi D\bar{D}$ and observed a new charmoniumlike structure $X^*(3860)$ with a significance of 6.5σ [5]. Using Monte Carlo simulation, Belle compared the $J^{PC}=0^{++}$ and 2^{++} hypotheses for the $X^*(3860)$ and found that the $J^{PC}=0^{++}$ hypothesis is favored, although the 2^{++} hypothesis is not excluded [5].

The masses and decay widths for the $X(4160)$, $Z(3930)$, $X(3915)$, $X(4350)$, and $X^*(3860)$ are shown in Table I. Their possible quantum numbers are also listed in the second column. According to the Godfrey-Isgur) model calculations [6,7], the $Z(3930)$ has been assigned as the 2^3P_2 radially excited charmonium $\chi'_{c2}(2P)$ with $J^{PC}=2^{++}$, while the $X(3915)$ has been assigned as the $\chi_{c0}(2P)$ charmonium state with $J^{PC}=0^{++}$ in PDG [8]. Such an assignment was also supported by analyzing the mass spectrum of the P-wave charmonium family and open-charm strong decay of the $X(3915)$ [9,10]. However, the $\chi_{c0}(2P)$ interpretation for $X(3915)$ was challenged by the absence of the $D\bar{D}$ decay mode and small mass splitting between $X(3915)$ and $Z(3930)$ compared with that between $\chi_{c0}(2P)$ and $\chi_{c2}(2P)$ [11]. In Ref. [5], Belle thus suggested the $X^*(3860)$ as a better candidate for the $\chi_{c0}(2P)$ charmonium state than $X(3915)$ since its mass and decay mode are well matched with the expectations for $\chi_{c0}(2P)$. This suggestion was studied in a Friedrichs model–like scheme in Ref. [12]. Additionally, the tetraquark interpretation was also proposed to study the nature of $X(3915)$ and $X^*(3860)$. In Ref. [13], the $X(3915)$ was considered as the lightest 0^{++} $cs\bar{c}\bar{s}$ tetraquark state in the diquark model. Such an interpretation was

*hxchen@buaa.edu.cn
†xiangliu@lzu.edu.cn
‡tom.steele@usask.ca
§zhusl@pku.edu.cn

TABLE I. Experimental parameters for $X(4160)$, $Z(3930)$, $X(3915)$, $X(4350)$, and $X^*(3860)$.

State	J^{PC}	Process	Mass (MeV)	Width (MeV)
$Z(3930)$ [1]	2^{++}	$\gamma\gamma \to D\bar{D}$	$3929 \pm 5 \pm 2$	$29 \pm 10 \pm 2$
$X(3915)$ [2]	0^{++} or 2^{++}	$\gamma\gamma \to \omega J/\psi$	$3915 \pm 3 \pm 2$ MeV	$17 \pm 10 \pm 3$
$X(4350)$ [3]	0^{++} or 2^{++}	$\gamma\gamma \to \phi J/\psi$	$4350.6^{+4.6}_{-5.1} \pm 0.7$ MeV	$13^{+18}_{-9} \pm 4$
$X(4160)$ [4]	$?^{?+}$	$e^+e^- \to J/\psi D^{*+}D^{*-}$	4156^{+29}_{-25}	37^{+27}_{-17}
$X^*(3860)$ [5]	0^{++} (prefered) or 2^{++}	$e^+e^- \to J/\psi D\bar{D}$	3862^{+26+40}_{-32-13}	$201^{+154+88}_{-67-82}$

supported by the QCD sum rule calculation [14]. See also QCD sum rule studies in Refs. [15–19]. The $X^*(3860)$ was explained to be the scalar $cs\bar{c}\bar{s}$ state in Refs. [20,21].

Since the $X(4160)$ was only observed in the $D^*\bar{D}^*$ final states [4], its J^P quantum numbers have not been determined up to now. In Ref. [22], Chao ruled out the interpretations of the $X(4160)$ as the $\psi(4160)$ or D-wave charmonium state 2^1D_2 with $J^{PC} = 2^{-+}$ based on Nonrelativistic Quantum Chromodynamics (NRQCD) calculations and proposed the $X(4160)$ as a candidate of the $\eta_c(4S)$. However, the $\eta_c(4S)$ assignment for the $X(4160)$ was in conflict with the mass and decay width predictions for $\eta_c(4S)$ state [7,23,24]. The $X(4160)$ was also explained as an isoscalar $D_s^*\bar{D}_s^*$ molecular state with $J^{PC} = 2^{++}$ within the framework of the hidden gauge formalism in Ref. [25]. See also discussions in Refs. [26–28].

In the recent reviews [29–33], one can consult the latest progress on the $X(4160)$, $X(3915)$, $X(4350)$, and $X^*(3860)$ states. The tetraquark configuration is an interesting explanation of their underlying structure. As shown in Table I, the quantum numbers for the $X(4160)$, $X(3915)$, $X(4350)$, and $X^*(3860)$ states can be $J^{PC} = 0^{++}$ or 2^{++}. In this paper, we shall study the mass spectra for the $qc\bar{q}\,\bar{c}$, $sc\bar{s}\,\bar{c}$, $qb\bar{q}\,\bar{b}$, and $sb\bar{s}\,\bar{b}$ tetraquark states with $J^{PC} = 0^{++}$ and 2^{++} in the method of QCD sum rules.

This paper is organized as follows. In Sec. II, we systematically construct the $qc\bar{q}\,\bar{c}$ tetraquark interpolating currents with $J^{PC} = 0^{++}$ and 2^{++} and introduce the QCD sum rule formalism. Then, we derive the spectral densities with the two-point correlation functions. In Sec. III, we perform the QCD sum rule analyses and extract the mass spectra of the $qc\bar{q}\bar{c}$, $sc\bar{s}\bar{c}$, $qb\bar{q}\bar{b}$, and $sb\bar{s}\bar{b}$ tetraquark states. The last section is a brief discussion and summary.

II. FORMALISM OF QCD SUM RULES

To explore the charmoniumlike tetraquark systems, we construct the $qc\bar{q}\bar{c}$ diquark-antidiquark operators using the diquark fields $q_a^TCc_b$, $q_a^TC\gamma_5c_b$, $q_a^TC\gamma_\mu c_b$, $q_a^TC\gamma_\mu\gamma_5c_b$, and $q_a^TC\sigma_{\mu\nu}c_b$ with various Lorentz structures [34–39]. Using SU(3) color symmetry, we obtain the scalar interpolating currents with quantum numbers $J^{PC} = 0^{++}$,

$$\begin{aligned}
J_1 &= q_a^TC\gamma_5c_b(\bar{q}_a\gamma_5C\bar{c}_b^T + \bar{q}_b\gamma_5C\bar{c}_a^T),\\
J_2 &= q_a^TC\gamma_\mu c_b(\bar{q}_a\gamma^\mu C\bar{c}_b^T + \bar{q}_b\gamma^\mu C\bar{c}_a^T),\\
J_3 &= q_a^TC\gamma_5c_b(\bar{q}_a\gamma_5C\bar{c}_b^T - \bar{q}_b\gamma_5C\bar{c}_a^T),\\
J_4 &= q_a^TC\gamma_\mu c_b(\bar{q}_a\gamma^\mu C\bar{c}_b^T - \bar{q}_b\gamma^\mu C\bar{c}_a^T),\\
J_5 &= q_a^TCc_b(\bar{q}_aC\bar{c}_b^T + \bar{q}_bC\bar{c}_a^T),\\
J_6 &= q_a^TC\gamma_\mu\gamma_5c_b(\bar{q}_a\gamma^\mu\gamma_5C\bar{c}_b^T + \bar{q}_b\gamma^\mu\gamma_5C\bar{c}_a^T),\\
J_7 &= q_a^TC\sigma_{\mu\nu}c_b(\bar{q}_a\sigma^{\mu\nu}C\bar{c}_b^T + \bar{q}_b\sigma^{\mu\nu}C\bar{c}_a^T),\\
J_8 &= q_a^TCc_b(\bar{q}_aC\bar{c}_b^T - \bar{q}_bC\bar{c}_a^T),\\
J_9 &= q_a^TC\gamma_\mu\gamma_5c_b(\bar{q}_a\gamma^\mu\gamma_5C\bar{c}_b^T - \bar{q}_b\gamma^\mu\gamma_5C\bar{c}_a^T),\\
J_{10} &= q_a^TC\sigma_{\mu\nu}c_b(\bar{q}_a\sigma^{\mu\nu}C\bar{c}_b^T - \bar{q}_b\sigma^{\mu\nu}C\bar{c}_a^T),
\end{aligned} \tag{1}$$

and the tensor interpolating currents with quantum numbers $J^{PC} = 2^{++}$,

$$\begin{aligned}
J_{11\mu\nu} &= q_a^TC\gamma_\mu c_b(\bar{q}_a\gamma_\nu C\bar{c}_b^T - \bar{q}_b\gamma_\nu C\bar{c}_a^T) + q_a^TC\gamma_\nu c_b(\bar{q}_a\gamma_\mu C\bar{c}_b^T - \bar{q}_b\gamma_\mu C\bar{c}_a^T),\\
J_{12\mu\nu} &= q_a^TC\gamma_\mu\gamma_5c_b(\bar{q}_a\gamma_\nu\gamma_5C\bar{c}_b^T - \bar{q}_b\gamma_\nu\gamma_5C\bar{c}_a^T) + q_a^TC\gamma_\nu\gamma_5c_b(\bar{q}_a\gamma_\mu\gamma_5C\bar{c}_b^T - \bar{q}_b\gamma_\mu\gamma_5C\bar{c}_a^T),\\
J_{13\mu\nu} &= q_a^TC\gamma_\mu c_b(\bar{q}_a\gamma_\nu C\bar{c}_b^T + \bar{q}_b\gamma_\nu C\bar{c}_a^T) + q_a^TC\gamma_\nu c_b(\bar{q}_a\gamma_\mu C\bar{c}_b^T + \bar{q}_b\gamma_\mu C\bar{c}_a^T),\\
J_{14\mu\nu} &= q_a^TC\gamma_\mu\gamma_5c_b(\bar{q}_a\gamma_\nu\gamma_5C\bar{c}_b^T + \bar{q}_b\gamma_\nu\gamma_5C\bar{c}_a^T) + q_a^TC\gamma_\nu\gamma_5c_b(\bar{q}_a\gamma_\mu\gamma_5C\bar{c}_b^T + \bar{q}_b\gamma_\mu\gamma_5C\bar{c}_a^T),
\end{aligned} \tag{2}$$

in which the currents $J_1(x)$, $J_2(x)$, $J_5(x)$, $J_6(x)$, $J_7(x)$, $J_{13\mu\nu}(x)$, and $J_{13\mu\nu}(x)$ belong to the $[\mathbf{6_c}]_{qc} \otimes [\bar{\mathbf{6}}_\mathbf{c}]_{\bar{q}\,\bar{c}}$ color symmetric representation while the currents $J_3(x)$, $J_4(x)$, $J_8(x)$, $J_9(x)$, $J_{10}(x)$, $J_{11\mu\nu}(x)$, and $J_{12\mu\nu}(x)$ belong to the $[\bar{\mathbf{3}}_\mathbf{c}]_{qc} \otimes [\mathbf{3_c}]_{\bar{q}\,\bar{c}}$ color antisymmetric representation. Throughout our calculation, we assume $m_u = m_d = 0$. Hence, the masses of the isoscalar and isovector tetraquark states with the same heavy-flavor content are degenerate.

We study the two-point correlation functions induced by the above scalar and tensor interpolating currents, respectively,

$$\Pi(q^2) = i\int d^4x e^{iq\cdot x}\langle 0|T[J(x)J^\dagger(0)]|0\rangle, \tag{3}$$

$$\Pi_{\mu\nu,\rho\sigma}(q^2) = i\int d^4x e^{iq\cdot x}\langle 0|T[J_{\mu\nu}(x)J^\dagger_{\rho\sigma}(0)]|0\rangle, \tag{4}$$

where the currents $J(x)$ and $J_{\mu\nu}(x)$ can couple to the corresponding hadronic states with the same quantum numbers,

$$\langle 0|J|X\rangle = f_S, \tag{5}$$

$$\langle 0|J_{\mu\nu}|X\rangle = f_T\epsilon_{\mu\nu} + \cdots, \tag{6}$$

in which $\epsilon_{\mu\nu}$ is the polarization tensor, and f_S and f_T are the coupling constants. The polarization tensor $\epsilon_{\mu\nu}$ in Eq. (6) represents the coupling to the spin-2 state. There also exist some other structures (represented by "$\cdots$") for spin-0 and spin-1 hadrons, which are omitted here. Accordingly, the correlation function for the tensor current in Eq. (4) can be written as

$$\Pi_{\mu\nu,\rho\sigma}(q^2) = \frac{1}{2}\left(\eta_{\mu\rho}\eta_{\nu\sigma} + \eta_{\mu\sigma}\eta_{\nu\rho} - \frac{2}{3}\eta_{\mu\nu}\eta_{\rho\sigma}\right)\Pi(q^2) + \cdots, \tag{7}$$

where $\eta_{\mu\nu} = q_\mu q_\nu/q^2 - g_{\mu\nu}$. At the hadronic level, this invariant function can be described by the dispersion relation

$$\Pi(q^2) = \frac{(q^2)^N}{\pi}\int_{4m_c^2}^{\infty}\frac{\mathrm{Im}\Pi(s)}{s^N(s-q^2-i\epsilon)}ds + \sum_{n=0}^{N-1}b_n(q^2)^n, \tag{8}$$

in which b_n are unknown subtraction constants. The imaginary part in the first term is defined as the spectral function and can be written as a sum over δ functions,

$$\begin{aligned}\rho(s) &\equiv \mathrm{Im}\Pi(s)/\pi = \sum_n \delta(s-m_n^2)\langle 0|J|n\rangle\langle n|J^\dagger|0\rangle \\ &= f_X^2\delta(s-m_X^2) + \text{continuum},\end{aligned} \tag{9}$$

where we adopt the single narrow pole plus continuum parametrization in the second step.

Using the operator product expansion (OPE) method, the correlation function can also be computed at the quark-gluonic level in the expression of various QCD condensates. Due to the quark-hadron duality, the correlation functions obtained at the hadronic and quark-gluonic levels must equal to each other, based on which one can establish QCD sum rules relating these two levels. After performing the Borel transform, the QCD sum rules read as functions of the continuum threshold s_0 and Borel parameter M_B^2,

$$\mathcal{L}_k(s_0, M_B^2) = f_X^2 m_X^{2k} e^{-m_X^2/M_B^2} = \int_{4m_c^2}^{s_0} ds e^{-s/M_B^2}\rho(s)s^k. \tag{10}$$

The mass of the lowest-lying hadron state can be extracted as

$$m_X(s_0, M_B^2) = \sqrt{\frac{\mathcal{L}_1(s_0, M_B^2)}{\mathcal{L}_0(s_0, M_B^2)}}. \tag{11}$$

In this paper, the spectral density in Eq. (10) is calculated up to dimension 8 at the leading order of α_s, including the perturbative term and various nonperturbative condensates. In Appendix A, we list the expressions of $\rho(s)$ for all interpolating currents in Eqs. (1) and (2).

III. NUMERICAL ANALYSIS

In this section, we perform numerical analyses using the parameters of quark masses and various QCD condensates [8,40–43],

$$\begin{aligned} m_u &= m_d = m_q = 0, \\ m_c(m_c) &= 1.27 \pm 0.03\ \text{GeV}, \\ m_b(m_b) &= 4.18^{+0.04}_{-0.03}\ \text{GeV}, \\ m_s(2\ \text{GeV}) &= (96^{+8}_{-4})\ \text{MeV}, \\ \langle\bar{q}q\rangle &= -(0.23 \pm 0.03)^3\ \text{GeV}^3, \\ \langle\bar{s}s\rangle &= (0.8 \pm 0.1)\langle\bar{q}q\rangle, \\ \langle\bar{q}g_s\sigma\cdot Gq\rangle &= -M_0^2\langle\bar{q}q\rangle, \\ \langle\bar{s}g_s\sigma\cdot Gs\rangle &= -M_0^2\langle\bar{s}s\rangle, \\ M_0^2 &= (0.8 \pm 0.2)\ \text{GeV}^2, \\ \langle g_s^2GG\rangle &= (0.48 \pm 0.14)\ \text{GeV}^4, \end{aligned} \tag{12}$$

in which the $\overline{\text{MS}}$ running heavy quark masses are adopted. The QCD sum rules in Eq. (10) are functions of the continuum threshold s_0 and Borel parameter M_B^2. The working ranges for these two parameters will affect the numerical sum rule analyses. The suitable working range (Borel window) of M_B^2 can be determined by the requirement of the OPE convergence and the pole contribution (PC). In our analyses, we use the following criteria to obtain the Borel windows and optimal values for s_0:

(1) Requiring the dominant nonperturbative contribution (quark condensate $\langle\bar{q}q\rangle$) to be less than at least one-half of the perturbative term leads to the lower bound on the Borel parameter. This ratio is adjusted as $1/3$ for the currents $J_7(x)$ and $J_{10}(x)$ since the

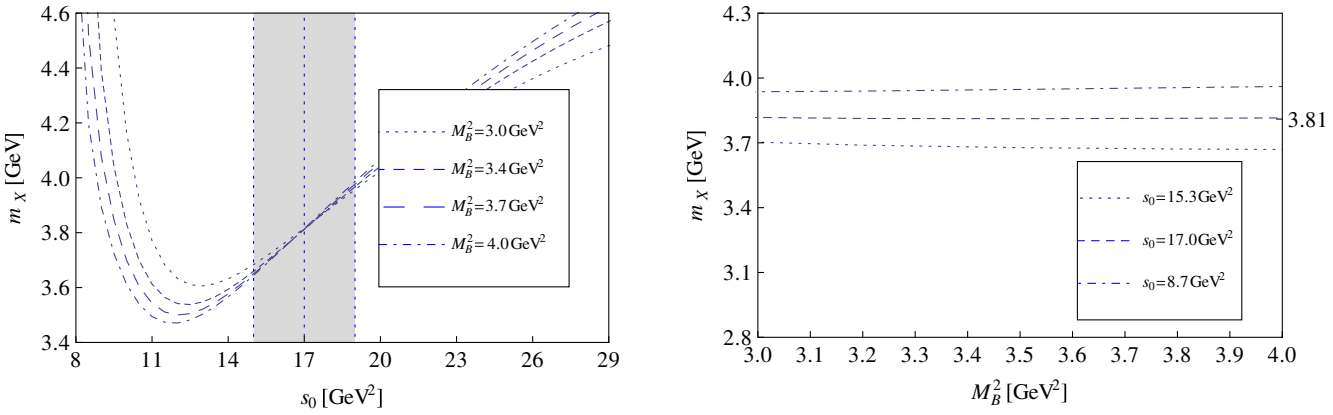

FIG. 1. Variations of the $qc\bar{q}\,\bar{c}$ hadron mass m_X with s_0 and M_B^2 for the $J^{PC}=0^{++}$ tetraquark using current $J_4(x)$.

quark condensate $\langle\bar{q}q\rangle$ and quark-gluon mixed condensate $\langle\bar{q}g_s\sigma\cdot Gq\rangle$ give no contribution in OPEs and thus the dimension-6 condensate $\langle\bar{q}q\rangle^2$ is the dominant power correction for these two channels.

(2) The contribution of the dimension-8 condensate $\langle\bar{q}q\rangle\langle\bar{q}g_s\sigma\cdot Gq\rangle$ should be less than 5%. This requirement can be usually satisfied under the first criterion except for the $J_7(x)$ and $J_{10}(x)$.

(3) We require the pole contribution to be larger than 10% [30% for $J_8(x)$] to restrict the upper bound on the Borel parameter, in which the PC is defined as

$$\mathrm{PC}\equiv\frac{\mathcal{L}_0(s_0,M_B^2)}{\mathcal{L}_0(\infty,M_B^2)}=\frac{\int_{4m_c^2}^{s_0}ds e^{-s/M_B^2}\rho(s)}{\int_{4m_c^2}^{\infty}ds e^{-s/M_B^2}\rho(s)}. \quad (13)$$

(4) By minimizing the dependence of m_X on M_B^2, we can determine the optimal value of s_0 in the Borel window.

The advantage of these criteria is that the working ranges for s_0 and M_B^2 can be determined by the intrinsic behavior of QCD sum rules itself. To show the behavior of the mass sum rules, we plot the variations of the extracted hadron mass with respect to s_0 and M_B^2 for the scalar current $J_4(x)$ in Fig. 1 as an example. Applying the above criteria, the Borel window for $J_4(x)$ is determined to be 3.0 GeV^2 $\leq M_B^2 \leq$ 4.0 GeV^2 with the optimal continuum threshold value $s_0 = 17.0$ GeV^2. One may find from the left side of Fig. 1 that the curves of m_X with different values of M_B^2 intersect around $s_0 = 17.0$ GeV^2, where the variation of m_X with M_B^2 is very weak. Considering 10% uncertainty of s_0, we can plot the Borel curves in the above Borel window, as shown in the right side of Fig 1. These Borel curves are very stable with respect to M_B^2, and thus we extract the hadron mass and coupling constant as

$$m_{X,0^{++}} = 3.81 \pm 0.19 \text{ GeV}, \quad (14)$$

$$f_{X,0^{++}} = 2.18 \times 10^{-2} \text{ GeV}^5, \quad (15)$$

which is in very good agreement with the experimental mass of the $X^*(3860)$ state.

Performing similar analyses, we study the mass sum rules for all interpolating currents in Eq. (1). We study the

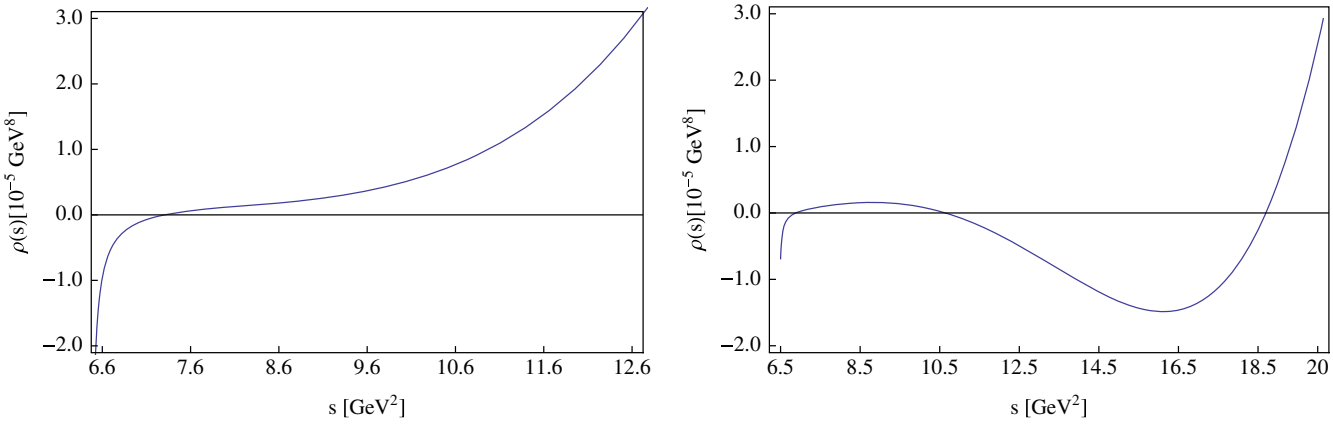

FIG. 2. Property of the spectral density for the interpolating currents $J_4(x)$ (left) and $J_8(x)$ (right) with $J^{PC}=0^{++}$.

TABLE II. Masses of the charmoniumlike $qc\bar{q}\bar{c}$ tetraquark states. The mass sum rules are unstable for the interpolating currents $J_5(x)$, $J_{12\mu\nu}(x)$, and $J_{14\mu\nu}(x)$.

J^{PC}	Currents	s_0 (GeV^2)	M_B^2 (GeV^2)	m_X (GeV)	PC	f_X (10^{-2} GeV^5)
0^{++}	J_1	20 ± 2.0	4.1–5.0	4.17 ± 0.20	13.9%	3.15
	J_2	15 ± 1.5	3.0–3.6	3.56 ± 0.17	14.4%	2.14
	J_3	16 ± 1.6	4.0–4.3	3.72 ± 0.17	9.41%	1.10
	J_4	17 ± 1.7	3.0–4.0	3.81 ± 0.19	15.9%	2.18
	J_7	15 ± 1.5	2.6–3.4	3.58 ± 0.18	16.0%	3.77
	J_9	19 ± 1.9	3.1–3.4	3.93 ± 0.19	12.2%	1.42
	J_{10}	18 ± 1.8	3.1–3.9	3.90 ± 0.16	14.4%	4.99
2^{++}	$J_{11\mu\nu}$	19 ± 1.9	4.2–4.8	4.06 ± 0.15	12.8%	11.0
	$J_{13\mu\nu}$	20 ± 2.0	4.2–5.1	4.16 ± 0.20	14.3%	18.6

properties of the spectral densities in Fig. 2. The spectral density for $J_4(x)$ becomes positive in the region $s > 7.5$ GeV^2. However, the behavior for the spectral density for $J_8(x)$ is more complicated, as shown in Fig. 2, which becomes positive only for $s > 18.5$ GeV^2. Such a spectral density is unphysical and cannot be used to make a reliable mass prediction. The situations are similar for the currents $J_5(x)$ and $J_6(x)$. We shall not make mass predictions using these currents. For the other interpolating currents, we perform the numerical analyses and collect the numerical results in Table II. The errors of m_X come from the uncertainties of charm quark mass, various condensates, and the continuum threshold s_0, in which the uncertainties from s_0 and the quark condensate are the dominant error sources. As shown in Table II, the masses extracted from $J_4(x)$, $J_9(x)$, and $J_{10}(x)$ are very close to the mass of $X^*(3860)$, which implies that these currents may couple well to this state and suggests a possible tetraquark interpretation for $X^*(3860)$.

For the tensor current $J_{11\mu\nu}$ with $J^{PC} = 2^{++}$, we show the variations of m_X with s_0 and M_B^2 in Fig. 3 and extract the mass and coupling constant as

$$m_{X,2^{++}} = 4.06 \pm 0.15 \text{ GeV}, \tag{16}$$

$$f_{X,2^{++}} = 0.11 \text{ GeV}^5, \tag{17}$$

which is a bit higher than the mass of $X^*(3860)$ but is still consistent with the experiment result within errors. Similarly, we can also study the hidden-charm $sc\bar{s}\,\bar{c}$ tetraquark systems in the same channels. Using the spectral densities in Appendix A, we can make the replacement $\langle\bar{q}q\rangle \to \langle\bar{s}s\rangle$ and $\langle\bar{q}g_s\sigma\cdot Gq\rangle \to \langle\bar{s}g_s\sigma\cdot Gs\rangle$. After performing similar numerical analyses, we collect the numerical results for the $sc\bar{s}\,\bar{c}$ tetraquark states in Table III. The masses for these $sc\bar{s}\,\bar{c}$ tetraquarks are almost degenerate with the $qc\bar{q}\,\bar{c}$ states with the same current. In QCD sum rule calculations, such a degeneracy always happens for the positive-parity hidden-flavor tetraquark systems [37]. This is very different from the situation of the negative-parity tetraquarks in which there is a 0.1–0.2 GeV mass difference between strange and nonstrange states [37]. Such a discrepancy happens due to different OPE behavior, in which the quark condensate $\langle\bar{q}q\rangle$ is dominant for positive-parity tetraquarks, while the four-quark condensate $\langle\bar{q}q\bar{q}q\rangle \sim \langle\bar{q}q\rangle^2$ is the most important nonperturbative contribution for the negative-parity systems [35–38].

With the heavy quark symmetry, we can similarly study the hidden-bottom $qb\bar{q}\bar{b}$ and $sb\bar{s}\,\bar{b}$ tetraquark states with

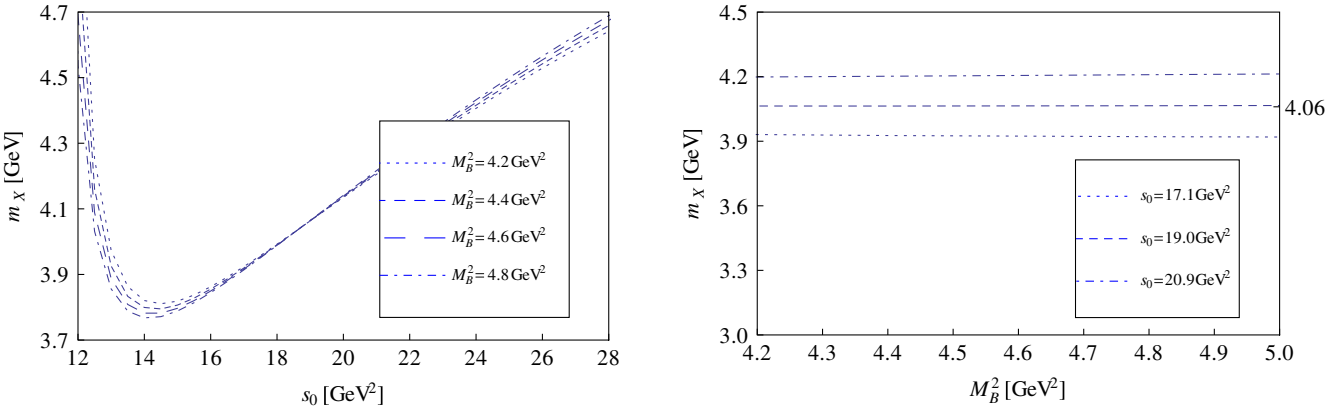

FIG. 3. Variations of the $qc\bar{q}\,\bar{c}$ hadron mass m_X with s_0 and M_B^2 for the $J^{PC} = 2^{++}$ tetraquark using current $J_{11\mu\nu}(x)$.

TABLE III. Masses of the charmoniumlike $sc\bar{s}\bar{c}$ tetraquark states.

J^{PC}	Currents	s_0 (GeV^2)	M_B^2 (GeV^2)	m_X (GeV)	PC	f_X (10^{-2} GeV^5)
0^{++}	J_1	20 ± 2.0	3.7–4.9	4.18 ± 0.19	14.8%	2.97
	J_2	15 ± 1.5	2.7–3.5	3.57 ± 0.15	15.5%	1.94
	J_3	16 ± 1.6	3.7–4.0	3.73 ± 0.17	10.6%	1.00
	J_4	17 ± 1.7	2.7–3.9	3.83 ± 0.19	17.0%	2.13
	J_7	16 ± 1.6	2.4–3.4	3.61 ± 0.15	19.1%	4.39
	J_9	18 ± 1.8	2.8–3.1	3.86 ± 0.15	13.4%	1.19
	J_{10}	18 ± 1.8	2.8–3.9	3.92 ± 0.17	16.1%	4.86
2^{++}	$J_{11\mu\nu}$	19 ± 1.9	3.8–4.7	4.07 ± 0.20	14.2%	10.3
	$J_{13\mu\nu}$	20 ± 2.0	3.8–5.0	4.17 ± 0.19	15.0%	17.5

TABLE IV. Masses of the bottomoniumlike $qb\bar{q}\bar{b}$ tetraquark states.

J^{PC}	Currents	s_0 (GeV^2)	M_B^2 (GeV^2)	m_X (GeV)	PC	f_X (10^{-1} GeV^5)
0^{++}	J_1	108 ± 5	9.3–9.9	10.00 ± 0.21	22.0%	1.51
	J_2	103 ± 5	7.4–8.8	9.71 ± 0.19	26.6%	1.82
	J_3	104 ± 5	9.2–9.5	9.83 ± 0.20	19.5%	0.82
	J_4	106 ± 5	7.6–9.2	9.87 ± 0.20	26.6%	1.59
	J_7	105 ± 5	7.6–8.4	9.80 ± 0.22	23.8%	4.03
	J_9	112 ± 5	8.2–8.5	10.18 ± 0.22	20.4%	1.56
	J_{10}	108 ± 5	8.0–8.9	9.96 ± 0.21	23.6%	3.65
2^{++}	$J_{11\mu\nu}$	108 ± 5	9.5–10.1	10.00 ± 0.21	21.8%	6.52
	$J_{13\mu\nu}$	109 ± 5	9.5–10.2	10.05 ± 0.22	22.7%	9.88

TABLE V. Masses of the bottomoniumlike $sb\bar{s}\bar{b}$ tetraquark states.

J^{PC}	Currents	s_0(GeV^2)	M_B^2 (GeV^2)	m_X (GeV)	PC	f_X (10^{-1} GeV^5)
0^{++}	J_1	108 ± 5	8.5–9.6	10.01 ± 0.21	24.5%	1.42
	J_2	103 ± 5	7.0–8.6	9.72 ± 0.19	28.3%	1.70
	J_3	104 ± 5	8.5–9.0	9.84 ± 0.20	21.8%	0.76
	J_4	106 ± 5	7.2–9.0	9.88 ± 0.19	27.4%	1.51
	J_7	105 ± 5	7.2–8.2	9.82 ± 0.20	25.1%	3.95
	J_9	111 ± 5	7.7–8.3	10.15 ± 0.21	22.2%	1.51
	J_{10}	108 ± 5	7.4–8.7	9.97 ± 0.19	26.1%	3.60
2^{++}	$J_{11\mu\nu}$	108 ± 5	8.7–9.8	10.01 ± 0.20	24.1%	6.14
	$J_{13\mu\nu}$	110 ± 5	8.7–10.2	10.09 ± 0.21	25.4%	9.97

$J^{PC} = 0^{++}$ and 2^{++}. Replacing $m_c \to m_b$ in the expressions of $\rho(s)$, we perform QCD sum rule analyses and collect the numerical results for the hidden-bottom $qb\bar{q}\bar{b}$ and $sb\bar{s}\bar{b}$ tetraquarks in Tables IV and V. One notes that the pole contributions and coupling constants for the hidden-bottom tetraquark systems are much higher than those in the hidden-charm systems. The masses for these hidden-bottom tetraquarks are around 9.7–10.2 GeV.

As shown above, the pole contributions of these tetraquark systems are very small due to the high dimension of the four-quark operators [36,37]. One may wonder if the mixed interpolating current can improve the pole contribution of the mass sum rule [44,45]. To study such a possibility, we have investigated some mixed operators by choosing any two currents in Eq. (1). We show our investigation by using the scalar mixed current as an example,

$$J^m = J_1 \cos\theta + J_4 \sin\theta, \tag{18}$$

where θ is a mixing angle. For this mixed current, one needs to calculate the mixed parts $\langle 0|T[J_1 J_4^\dagger]|0\rangle + \langle 0|T[J_4 J_1^\dagger]|0\rangle$ in the correlation function. As shown in Eq. (A13), the perturbative terms, quark condensate, and four-quark condensate in these mixed parts give no contributions to the correlation functions.

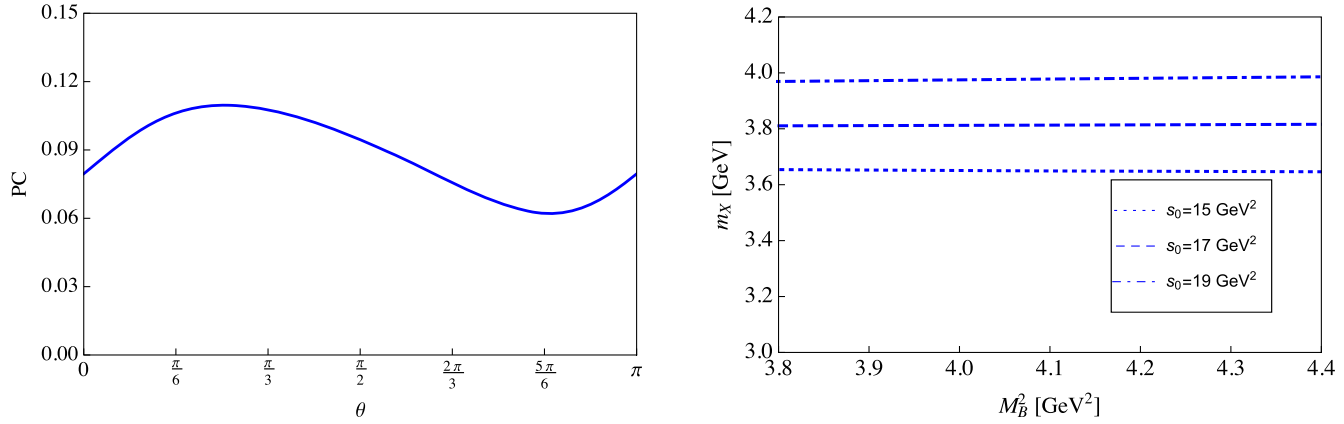

FIG. 4. Left: θ effect for pole contribution with $s_0 = 17$ GeV^2 and $M_B^2 = 4.1$ GeV^2. Right: Variations of hadron mass m_X with M_B^2.

Under the same QCD sum rule criteria, we obtain the Borel window $3.9\ \text{GeV}^2 \leq M_B^2 \leq 4.2\ \text{GeV}^2$ with $s_0 = 17\ \text{GeV}^2$. We show the θ effect for the pole contribution in the left panel of Fig. 4 with $s_0 = 17\ \text{GeV}^2$ and $M_B^2 = 4.1\ \text{GeV}^2$. It shows that the mixed current can only slightly improve the pole contribution for the mixing angle $\theta \approx 0.8$. The mass curves in the above parameter ranges are shown in the right panel of Fig. 4. Finally, we extract the hadron mass around 3.82 GeV, which is very close to the result from J_4.

IV. DISCUSSION AND SUMMARY

In this work, we have studied the hidden-charm/bottom $qc\bar{q}\bar{c}$, $sc\bar{s}\bar{c}$ and $qb\bar{q}\bar{b}$, $sb\bar{s}\bar{b}$ tetraquark systems in the method of QCD sum rules. We have constructed the interpolating tetraquark currents with $J^{PC} = 0^{++}$ and 2^{++} in a systematical way and calculated their correlation functions and spectral densities at the leading order on α_s. The mass spectra for these scalar and tensor tetraquark states are predicted. Since the quantum numbers for the $X(4160)$, $X(3915)$, $X(4350)$, and $X^*(3860)$ can be $J^{PC} = 0^{++}$ or 2^{++}, we can compare the experimental results for these resonances with the tetraquark mass spectra listed in Tables II and III.

In Fig. 5, we show the mass spectra for the hidden-charm $qc\bar{q}\bar{c}$ and $sc\bar{s}\bar{c}$ tetraquark states labeled by the interpolating current and J^{PC} quantum numbers. To compare these mass spectra with the masses of the $X(4160)$, $X(3915)$, $X(4350)$, and $X^*(3860)$, we also show their experimental mass values with uncertainties in Fig. 5.

For the hidden-charm $qc\bar{q}\bar{c}$ systems, the currents $J_4(x)$, $J_9(x)$, and $J_{10}(x)$ belong to the $[\bar{\mathbf{3}}_\mathbf{c}]_{\text{qc}} \otimes [\mathbf{3}_\mathbf{c}]_{\bar{q}\,\bar{c}}$ color antisymmetric representation. The isovector and isoscalar tetraquark masses extracted from these three currents are about 3.8–3.9 GeV, which is consistent with the mass of the $X^*(3860)$ state, as shown in Fig. 5. However, the isoscalar tetraquark currents composed of two S-wave diquarks may also couple to a conventional charmonium, especially the radially excited charmonium. For example, the light tetraquark currents may also couple to the conventional nonexotica physical states [46]. In other words, $X^*(3860)$ may be either an isoscalar tetraquark state or $\chi_{c0}(2P)$.

In contrast, the masses for the tensor charmoniumlike tetraquarks are about 4.06–4.16 GeV, which is a bit higher than that of $X^*(3860)$ but with a small overlap within errors. On the other hand, our results prefer the $J^{PC} = 0^{++}$ assignment for the $X^*(3860)$ over the 2^{++} assignment, which is also in agreement with the Belle experiment [5]. Nonetheless, the 2^{++} possibility is still not excluded as shown in Fig. 5.

Using the currents $J_1(x)$ with $J^{PC} = 0^{++}$ and $J_{13\mu\nu}(x)$ with $J^{PC} = 2^{++}$, we extract the hadron masses for the scalar and tensor $qc\bar{q}\bar{c}$ tetraquarks around 4.1–4.2 GeV. These results are in good agreement with the mass of the $X(4160)$ state, which implies the tetraquark interpretation for this resonance. For the $X(3915)$, our results favor the 0^{++} $qc\bar{q}\bar{c}$ or $sc\bar{s}\bar{c}$ tetraquark assignment over the tensor

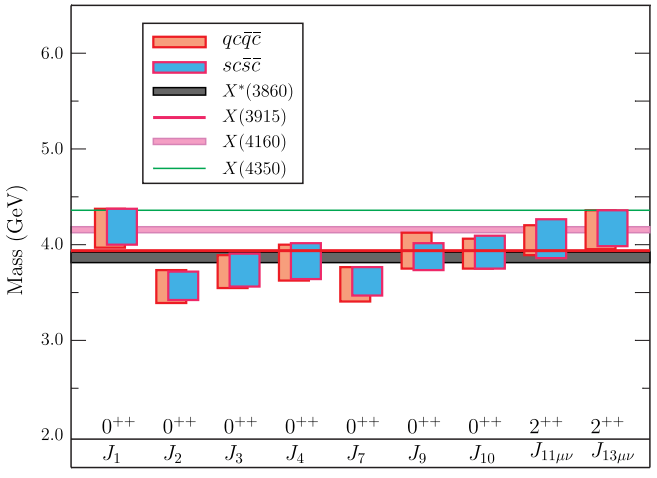

FIG. 5. Mass spectra for the hidden-charm $qc\bar{q}\bar{c}$ and $sc\bar{s}\bar{c}$ tetraquark states with $J^{PC} = 0^{++}$ and 2^{++}. The vertical sizes of the rectangles represent the uncertainties of the experimental hadron masses and our calculations.

assignment. From Fig. 5, the $qc\bar{q}\bar{c}$ and $sc\bar{s}\bar{c}$ tetraquarks are almost degenerate for the same interpolating current and quantum numbers. Our results do not support the $X(4350)$ to be a $sc\bar{s}\bar{c}$ tetraquark with $J^{PC}=0^{++}$ or 2^{++}. We have also predicted the mass spectra of the hidden-bottom $qb\bar{q}\bar{b}$ and $sb\bar{s}\bar{b}$ tetraquarks with $J^{PC}=0^{++}$ and 2^{++}. The masses for these hidden-bottom tetraquarks are obtained around 9.7–10.2 GeV. These mass predictions may be useful for understanding the tetraquark spectroscopy and searching for such states at the facilities such as LHCb and BelleII in the future.

ACKNOWLEDGMENTS

This project is supported by the Natural Sciences and Engineering Research Council of Canada (NSERC); the Chinese National Youth Thousand Talents Program; the National Natural Science Foundation of China under Grants No. 11475015, No. 11375024, No. 11222547, No. 11175073, No. 11575008, and No. 11621131001; the 973 program; the Ministry of Education of China (SRFDP under Grant No. 20120211110002 and the Fundamental Research Funds for the Central Universities); and the National Program for Support of Top-Notch Youth Professionals.

APPENDIX: THE SPECTRAL DENSITIES

In this appendix, we list the expressions of the spectral densities for the interpolating currents listed in Eqs. (1) and (2) as follows. The spectral densities are calculated by including the perturbative term, quark condensate $\langle\bar{q}q\rangle$, gluon condensate $\langle g_s^2GG\rangle$, quark-gluon mixed condensate $\langle\bar{q}g_s\sigma\cdot Gq\rangle$, four-quark condensate $\langle\bar{q}q\rangle^2$, and dimension-8 condensate $\langle\bar{q}q\rangle\langle\bar{q}g_s\sigma\cdot Gq\rangle$,

$$\rho_i(s)=\rho_i^{\rm pert}(s)+\rho_i^{\langle\bar{q}q\rangle}(s)+\rho_i^{\langle GG\rangle}(s)+\rho_i^{\langle\bar{q}Gq\rangle}(s)+\rho_i^{\langle\bar{q}q\rangle^2}(s)+\rho_i^{\langle\bar{q}q\rangle\langle\bar{q}Gq\rangle}(s), \tag{A1}$$

in which the subscript "i" denotes the interpolating current number.

For the current J_1 with $J^{PC}=0^{++}$,

$$\begin{aligned}
\rho_1^{\rm pert}(s)&=\frac{1}{256\pi^6}\int_{\alpha_{\rm min}}^{\alpha_{\rm max}}d\alpha\int_{\beta_{\rm min}}^{\beta_{\rm max}}d\beta\frac{(1-\alpha-\beta)^2[m_c^2(\alpha+\beta)-3\alpha\beta s][(\alpha+\beta)m_c^2-\alpha\beta s]^3}{\alpha^3\beta^3},\\
\rho_1^{\langle\bar{q}q\rangle}(s)&=-\frac{m_c\langle\bar{q}q\rangle}{4\pi^4}\int_{\alpha_{\rm min}}^{\alpha_{\rm max}}d\alpha\int_{\beta_{\rm min}}^{\beta_{\rm max}}d\beta\frac{(1-\alpha-\beta)[(\alpha+\beta)m_c^2-\alpha\beta s][m_c^2(\alpha+\beta)-2\alpha\beta s]}{\alpha^2\beta},\\
\rho_1^{\langle GG\rangle}(s)&=\frac{\langle g_s^2GG\rangle}{256\pi^6}\int_{\alpha_{\rm min}}^{\alpha_{\rm max}}d\alpha\int_{\beta_{\rm min}}^{\beta_{\rm max}}d\beta\left\{\frac{m_c^2(1-\alpha-\beta)^2[2m_c^2(\alpha+\beta)-3\alpha\beta s]}{3\beta^3}\right.\\
&\quad\left.-\frac{(1-\alpha-\beta)[m_c^2(\alpha+\beta)-2\alpha\beta s][(\alpha+\beta)m_c^2-\alpha\beta s]}{2\alpha\beta^2}\right\},\\
\rho_1^{\langle\bar{q}Gq\rangle}(s)&=\frac{m_c\langle\bar{q}g_s\sigma\cdot Gq\rangle}{32\pi^4}\int_{\alpha_{\rm min}}^{\alpha_{\rm max}}d\alpha\int_{\beta_{\rm min}}^{\beta_{\rm max}}d\beta\frac{(1+\alpha-\beta)[2m_c^2(\alpha+\beta)-3\alpha\beta s]}{\alpha^2},\\
\rho_1^{\langle\bar{q}q\rangle^2}(s)&=\frac{m_c^2\langle\bar{q}q\rangle^2}{6\pi^2}\sqrt{1-4m_c^2/s},\\
\rho_1^{\langle\bar{q}q\rangle\langle\bar{q}Gq\rangle}(s)&=\frac{m_c^2\langle\bar{q}q\rangle\langle\bar{q}g_s\sigma\cdot Gq\rangle}{24\pi^2}\int_0^1 d\alpha\left\{\frac{2m_c^2}{\alpha^2}\delta'(s-\tilde{m}_c^2)+\frac{1}{\alpha}\delta(s-\tilde{m}_c^2)\right\},
\end{aligned} \tag{A2}$$

where the integral limits are

$$\alpha_{\rm max}=\frac{1+\sqrt{1-4m_c^2/s}}{2},\qquad \alpha_{\rm min}=\frac{1-\sqrt{1-4m_c^2/s}}{2},\qquad \beta_{\rm max}=1-\alpha,\qquad \beta_{\rm min}=\frac{\alpha m_c^2}{\alpha s-m_c^2}. \tag{A3}$$

For the current J_2 with $J^{PC}=0^{++}$,

$$\begin{aligned}
\rho_2^{\rm pert}(s) &= \frac{1}{64\pi^6}\int_{\alpha_{\rm min}}^{\alpha_{\rm max}} d\alpha \int_{\beta_{\rm min}}^{\beta_{\rm max}} d\beta \frac{(1-\alpha-\beta)^2[m_c^2(\alpha+\beta)-3\alpha\beta s][(\alpha+\beta)m_c^2-\alpha\beta s]^3}{\alpha^3\beta^3},\\
\rho_2^{\langle\bar{q}q\rangle}(s) &= -\frac{m_c\langle\bar{q}q\rangle}{2\pi^4}\int_{\alpha_{\rm min}}^{\alpha_{\rm max}} d\alpha \int_{\beta_{\rm min}}^{\beta_{\rm max}} d\beta \frac{(1-\alpha-\beta)[(\alpha+\beta)m_c^2-\alpha\beta s][m_c^2(\alpha+\beta)-2\alpha\beta s]}{\alpha^2\beta},\\
\rho_2^{\langle GG\rangle}(s) &= \frac{\langle g_s^2 GG\rangle}{64\pi^6}\int_{\alpha_{\rm min}}^{\alpha_{\rm max}} d\alpha \int_{\beta_{\rm min}}^{\beta_{\rm max}} d\beta \Bigg\{\frac{m_c^2(1-\alpha-\beta)^2[2m_c^2(\alpha+\beta)-3\alpha\beta s]}{3\beta^3}\\
&\quad + \frac{5[m_c^2(\alpha+\beta)-2\alpha\beta s][(\alpha+\beta)m_c^2-\alpha\beta s]}{16}\left[\frac{(1-\alpha-\beta)^2}{2\alpha^2\beta^2}+\frac{(2-2\alpha-\beta)}{\alpha\beta^2}\right]\Bigg\},\\
\rho_2^{\langle\bar{q}Gq\rangle}(s) &= -\frac{m_c\langle\bar{q}g_s\sigma\cdot Gq\rangle}{64\pi^4}\int_{\alpha_{\rm min}}^{\alpha_{\rm max}} d\alpha \int_{\beta_{\rm min}}^{\beta_{\rm max}} d\beta \frac{(5-13\beta)[2m_c^2(\alpha+\beta)-3\alpha\beta s]}{\alpha\beta},\\
\rho_2^{\langle\bar{q}q\rangle^2}(s) &= \frac{2m_c^2\langle\bar{q}q\rangle^2}{3\pi^2}\sqrt{1-4m_c^2/s},\\
\rho_2^{\langle\bar{q}q\rangle\langle\bar{q}Gq\rangle}(s) &= \frac{m_c^2\langle\bar{q}q\rangle\langle\bar{q}g_s\sigma\cdot Gq\rangle}{24\pi^2}\int_0^1 d\alpha\left\{\frac{8m_c^2}{\alpha^2}\delta'(s-\tilde{m}_c^2)-\frac{5}{\alpha}\delta(s-\tilde{m}_c^2)\right\}.
\end{aligned} \tag{A4}$$

For the current J_3 with $J^{PC}=0^{++}$,

$$\begin{aligned}
\rho_3^{\rm pert}(s) &= \frac{1}{512\pi^6}\int_{\alpha_{\rm min}}^{\alpha_{\rm max}} d\alpha \int_{\beta_{\rm min}}^{\beta_{\rm max}} d\beta \frac{(1-\alpha-\beta)^2[m_c^2(\alpha+\beta)-3\alpha\beta s][(\alpha+\beta)m_c^2-\alpha\beta s]^3}{\alpha^3\beta^3},\\
\rho_3^{\langle\bar{q}q\rangle}(s) &= -\frac{m_c\langle\bar{q}q\rangle}{8\pi^4}\int_{\alpha_{\rm min}}^{\alpha_{\rm max}} d\alpha \int_{\beta_{\rm min}}^{\beta_{\rm max}} d\beta \frac{(1-\alpha-\beta)[(\alpha+\beta)m_c^2-\alpha\beta s][m_c^2(\alpha+\beta)-2\alpha\beta s]}{\alpha^2\beta},\\
\rho_3^{\langle GG\rangle}(s) &= \frac{\langle g_s^2 GG\rangle}{512\pi^6}\int_{\alpha_{\rm min}}^{\alpha_{\rm max}} d\alpha \int_{\beta_{\rm min}}^{\beta_{\rm max}} d\beta \Bigg\{\frac{m_c^2(1-\alpha-\beta)^2[2m_c^2(\alpha+\beta)-3\alpha\beta s]}{3\beta^3}\\
&\quad + \frac{(1-\alpha-\beta)[m_c^2(\alpha+\beta)-2\alpha\beta s][(\alpha+\beta)m_c^2-\alpha\beta s]}{\alpha\beta^2}\Bigg\},\\
\rho_3^{\langle\bar{q}Gq\rangle}(s) &= -\frac{m_c\langle\bar{q}g_s\sigma\cdot Gq\rangle}{32\pi^4}\int_{\alpha_{\rm min}}^{\alpha_{\rm max}} d\alpha \int_{\beta_{\rm min}}^{\beta_{\rm max}} d\beta \frac{(1-2\alpha-\beta)[2m_c^2(\alpha+\beta)-3\alpha\beta s]}{\alpha^2},\\
\rho_3^{\langle\bar{q}q\rangle^2}(s) &= \frac{m_c^2\langle\bar{q}q\rangle^2}{12\pi^2}\sqrt{1-4m_c^2/s},\\
\rho_3^{\langle\bar{q}q\rangle\langle\bar{q}Gq\rangle}(s) &= \frac{m_c^2\langle\bar{q}q\rangle\langle\bar{q}g_s\sigma\cdot Gq\rangle}{24\pi^2}\int_0^1 d\alpha\left\{\frac{m_c^2}{\alpha^2}\delta'(s-\tilde{m}_c^2)-\frac{1}{\alpha}\delta(s-\tilde{m}_c^2)\right\}.
\end{aligned} \tag{A5}$$

For the current J_4 with $J^{PC}=0^{++}$,

$$\begin{aligned}
\rho_4^{\text{pert}}(s) &= \frac{1}{128\pi^6}\int_{\alpha_{\min}}^{\alpha_{\max}} d\alpha \int_{\beta_{\min}}^{\beta_{\max}} d\beta \frac{(1-\alpha-\beta)^2[m_c^2(\alpha+\beta)-3\alpha\beta s][(\alpha+\beta)m_c^2-\alpha\beta s]^3}{\alpha^3\beta^3},\\
\rho_4^{\langle\bar{q}q\rangle}(s) &= -\frac{m_c\langle\bar{q}q\rangle}{4\pi^4}\int_{\alpha_{\min}}^{\alpha_{\max}} d\alpha \int_{\beta_{\min}}^{\beta_{\max}} d\beta \frac{(1-\alpha-\beta)[(\alpha+\beta)m_c^2-\alpha\beta s][m_c^2(\alpha+\beta)-2\alpha\beta s]}{\alpha^2\beta},\\
\rho_4^{\langle GG\rangle}(s) &= \frac{\langle g_s^2 GG\rangle}{128\pi^6}\int_{\alpha_{\min}}^{\alpha_{\max}} d\alpha \int_{\beta_{\min}}^{\beta_{\max}} d\beta \left\{\frac{m_c^2(1-\alpha-\beta)^2[2m_c^2(\alpha+\beta)-3\alpha\beta s]}{3\beta^3}\right.\\
&\quad \left.+\frac{[m_c^2(\alpha+\beta)-2\alpha\beta s][(\alpha+\beta)m_c^2-\alpha\beta s]}{8}\left[\frac{(1-\alpha-\beta)^2}{2\alpha^2\beta^2}+\frac{(2-2\alpha-\beta)}{\alpha\beta^2}\right]\right\},\\
\rho_4^{\langle\bar{q}Gq\rangle}(s) &= -\frac{m_c\langle\bar{q}g_s\sigma\cdot Gq\rangle}{64\pi^4}\int_{\alpha_{\min}}^{\alpha_{\max}} d\alpha \int_{\beta_{\min}}^{\beta_{\max}} d\beta \frac{(1-5\beta)[2m_c^2(\alpha+\beta)-3\alpha\beta s]}{\alpha\beta},\\
\rho_4^{\langle\bar{q}q\rangle^2}(s) &= \frac{m_c^2\langle\bar{q}q\rangle^2}{3\pi^2}\sqrt{1-4m_c^2/s},\\
\rho_4^{\langle\bar{q}q\rangle\langle\bar{q}Gq\rangle}(s) &= \frac{m_c^2\langle\bar{q}q\rangle\langle\bar{q}g_s\sigma\cdot Gq\rangle}{24\pi^2}\int_0^1 d\alpha\left\{\frac{4m_c^2}{\alpha^2}\delta'(s-\tilde{m}_c^2)-\frac{1}{\alpha}\delta(s-\tilde{m}_c^2)\right\}.
\end{aligned} \tag{A6}$$

For the current J_5 with $J^{PC}=0^{++}$,

$$\begin{aligned}
\rho_5^{pert}(s) &= \frac{1}{256\pi^6}\int_{\alpha_{\min}}^{\alpha_{\max}} d\alpha \int_{\beta_{\min}}^{\beta_{\max}} d\beta \frac{(1-\alpha-\beta)^2[m_c^2(\alpha+\beta)-3\alpha\beta s][(\alpha+\beta)m_c^2-\alpha\beta s]^3}{\alpha^3\beta^3},\\
\rho_5^{\langle\bar{q}q\rangle}(s) &= \frac{m_c\langle\bar{q}q\rangle}{4\pi^4}\int_{\alpha_{\min}}^{\alpha_{\max}} d\alpha \int_{\beta_{\min}}^{\beta_{\max}} d\beta \frac{(1-\alpha-\beta)[(\alpha+\beta)m_c^2-\alpha\beta s][m_c^2(\alpha+\beta)-2\alpha\beta s]}{\alpha^2\beta},\\
\rho_5^{\langle GG\rangle}(s) &= \frac{\langle g_s^2 GG\rangle}{256\pi^6}\int_{\alpha_{\min}}^{\alpha_{\max}} d\alpha \int_{\beta_{\min}}^{\beta_{\max}} d\beta \left\{\frac{m_c^2(1-\alpha-\beta)^2[2m_c^2(\alpha+\beta)-3\alpha\beta s]}{3\beta^3}\right.\\
&\quad \left.-\frac{(1-\alpha-\beta)[m_c^2(\alpha+\beta)-2\alpha\beta s][(\alpha+\beta)m_c^2-\alpha\beta s]}{2\alpha\beta^2}\right\},\\
\rho_5^{\langle\bar{q}Gq\rangle}(s) &= -\frac{m_c\langle\bar{q}g_s\sigma\cdot Gq\rangle}{32\pi^4}\int_{\alpha_{\min}}^{\alpha_{\max}} d\alpha \int_{\beta_{\min}}^{\beta_{\max}} d\beta \frac{(1+\alpha-\beta)[2m_c^2(\alpha+\beta)-3\alpha\beta s]}{\alpha^2},\\
\rho_5^{\langle\bar{q}q\rangle^2}(s) &= \frac{m_c^2\langle\bar{q}q\rangle^2}{6\pi^2}\sqrt{1-4m_c^2/s},\\
\rho_5^{\langle\bar{q}q\rangle\langle\bar{q}Gq\rangle}(s) &= \frac{m_c^2\langle\bar{q}q\rangle\langle\bar{q}g_s\sigma\cdot Gq\rangle}{24\pi^2}\int_0^1 d\alpha\left\{\frac{2m_c^2}{\alpha^2}\delta'(s-\tilde{m}_c^2)+\frac{1}{\alpha}\delta(s-\tilde{m}_c^2)\right\}.
\end{aligned} \tag{A7}$$

For the current J_6 with $J^{PC}=0^{++}$,

$$\rho_6^{\rm pert}(s)=\frac{1}{64\pi^6}\int_{\alpha_{\rm min}}^{\alpha_{\rm max}}d\alpha\int_{\beta_{\rm min}}^{\beta_{\rm max}}d\beta\frac{(1-\alpha-\beta)^2[m_c^2(\alpha+\beta)-3\alpha\beta s][(\alpha+\beta)m_c^2-\alpha\beta s]^3}{\alpha^3\beta^3},$$
$$\rho_6^{\langle\bar{q}q\rangle}(s)=\frac{m_c\langle\bar{q}q\rangle}{2\pi^4}\int_{\alpha_{\rm min}}^{\alpha_{\rm max}}d\alpha\int_{\beta_{\rm min}}^{\beta_{\rm max}}d\beta\frac{(1-\alpha-\beta)[(\alpha+\beta)m_c^2-\alpha\beta s][m_c^2(\alpha+\beta)-2\alpha\beta s]}{\alpha^2\beta},$$
$$\rho_6^{\langle GG\rangle}(s)=\frac{\langle g_s^2GG\rangle}{64\pi^6}\int_{\alpha_{\rm min}}^{\alpha_{\rm max}}d\alpha\int_{\beta_{\rm min}}^{\beta_{\rm max}}d\beta\Bigg\{\frac{m_c^2(1-\alpha-\beta)^2[2m_c^2(\alpha+\beta)-3\alpha\beta s]}{3\beta^3}$$
$$+\frac{5[m_c^2(\alpha+\beta)-2\alpha\beta s][(\alpha+\beta)m_c^2-\alpha\beta s]}{16}\left[\frac{(1-\alpha-\beta)^2}{2\alpha^2\beta^2}+\frac{(2-2\alpha-\beta)}{\alpha\beta^2}\right]\Bigg\},$$
$$\rho_6^{\langle\bar{q}Gq\rangle}(s)=\frac{m_c\langle\bar{q}g_s\sigma\cdot Gq\rangle}{64\pi^4}\int_{\alpha_{\rm min}}^{\alpha_{\rm max}}d\alpha\int_{\beta_{\rm min}}^{\beta_{\rm max}}d\beta\frac{(5-13\beta)[2m_c^2(\alpha+\beta)-3\alpha\beta s]}{\alpha\beta},$$
$$\rho_6^{\langle\bar{q}q\rangle^2}(s)=\frac{2m_c^2\langle\bar{q}q\rangle^2}{3\pi^2}\sqrt{1-4m_c^2/s},$$
$$\rho_6^{\langle\bar{q}q\rangle\langle\bar{q}Gq\rangle}(s)=\frac{m_c^2\langle\bar{q}q\rangle\langle\bar{q}g_s\sigma\cdot Gq\rangle}{24\pi^2}\int_0^1 d\alpha\left\{\frac{8m_c^2}{\alpha^2}\delta'(s-\tilde{m}_c^2)-\frac{5}{\alpha}\delta(s-\tilde{m}_c^2)\right\}. \tag{A8}$$

For the current J_7 with $J^{PC}=0^{++}$,

$$\rho_7^{pert}(s)=\frac{3}{32\pi^6}\int_{\alpha_{\rm min}}^{\alpha_{\rm max}}d\alpha\int_{\beta_{\rm min}}^{\beta_{\rm max}}d\beta\frac{(1-\alpha-\beta)^2[m_c^2(\alpha+\beta)-3\alpha\beta s][(\alpha+\beta)m_c^2-\alpha\beta s]^3}{\alpha^3\beta^3},$$
$$\rho_7^{\langle\bar{q}q\rangle}(s)=\rho_7^{\langle\bar{q}Gq\rangle}(s)=0,$$
$$\rho_7^{\langle GG\rangle}(s)=\frac{\langle g_s^2GG\rangle}{32\pi^6}\int_{\alpha_{\rm min}}^{\alpha_{\rm max}}d\alpha\int_{\beta_{\rm min}}^{\beta_{\rm max}}d\beta\Bigg\{\frac{m_c^2(1-\alpha-\beta)^2[2m_c^2(\alpha+\beta)-3\alpha\beta s]}{\beta^3}$$
$$+\frac{[m_c^2(\alpha+\beta)-2\alpha\beta s][(\alpha+\beta)m_c^2-\alpha\beta s]}{4}\left[\frac{5(1-\alpha-\beta)^2}{2\alpha^2\beta^2}+\frac{(12-12\alpha-7\beta)}{\alpha\beta^2}\right]\Bigg\},$$
$$\rho_7^{\langle\bar{q}q\rangle^2}(s)=\frac{4m_c^2\langle\bar{q}q\rangle^2}{\pi^2}\sqrt{1-4m_c^2/s},$$
$$\rho_7^{\langle\bar{q}q\rangle\langle\bar{q}Gq\rangle}(s)=\frac{2m_c^2\langle\bar{q}q\rangle\langle\bar{q}g_s\sigma\cdot Gq\rangle}{\pi^2}\int_0^1 d\alpha\left\{\frac{m_c^2}{\alpha^2}\delta'(s-\tilde{m}_c^2)-\frac{1}{\alpha}\delta(s-\tilde{m}_c^2)\right\}. \tag{A9}$$

For the current J_8 with $J^{PC}=0^{++}$,

$$\begin{aligned}
\rho_8^{pert}(s) &= \frac{1}{512\pi^6}\int_{\alpha_{\min}}^{\alpha_{\max}} d\alpha \int_{\beta_{\min}}^{\beta_{\max}} d\beta \frac{(1-\alpha-\beta)^2[m_c^2(\alpha+\beta)-3\alpha\beta s][(\alpha+\beta)m_c^2-\alpha\beta s]^3}{\alpha^3\beta^3},\\
\rho_8^{\langle\bar{q}q\rangle}(s) &= \frac{m_c\langle\bar{q}q\rangle}{8\pi^4}\int_{\alpha_{\min}}^{\alpha_{\max}} d\alpha \int_{\beta_{\min}}^{\beta_{\max}} d\beta \frac{(1-\alpha-\beta)[(\alpha+\beta)m_c^2-\alpha\beta s][m_c^2(\alpha+\beta)-2\alpha\beta s]}{\alpha^2\beta},\\
\rho_8^{\langle GG\rangle}(s) &= \frac{\langle g_s^2 GG\rangle}{512\pi^6}\int_{\alpha_{\min}}^{\alpha_{\max}} d\alpha \int_{\beta_{\min}}^{\beta_{\max}} d\beta \left\{\frac{m_c^2(1-\alpha-\beta)^2[2m_c^2(\alpha+\beta)-3\alpha\beta s]}{3\beta^3}\right.\\
&\quad \left.+\frac{(1-\alpha-\beta)[m_c^2(\alpha+\beta)-2\alpha\beta s][(\alpha+\beta)m_c^2-\alpha\beta s]}{\alpha\beta^2}\right\},\\
\rho_8^{\langle\bar{q}Gq\rangle}(s) &= \frac{m_c\langle\bar{q}g_s\sigma\cdot Gq\rangle}{32\pi^4}\int_{\alpha_{\min}}^{\alpha_{\max}} d\alpha \int_{\beta_{\min}}^{\beta_{\max}} d\beta \frac{(1-2\alpha-\beta)[2m_c^2(\alpha+\beta)-3\alpha\beta s]}{\alpha^2},\\
\rho_8^{\langle\bar{q}q\rangle^2}(s) &= \frac{m_c^2\langle\bar{q}q\rangle^2}{12\pi^2}\sqrt{1-4m_c^2/s},\\
\rho_8^{\langle\bar{q}q\rangle\langle\bar{q}Gq\rangle}(s) &= \frac{m_c^2\langle\bar{q}q\rangle\langle\bar{q}g_s\sigma\cdot Gq\rangle}{24\pi^2}\int_0^1 d\alpha\left\{\frac{m_c^2}{\alpha^2}\delta'(s-\tilde{m}_c^2)-\frac{1}{\alpha}\delta(s-\tilde{m}_c^2)\right\}.
\end{aligned} \tag{A10}$$

For the current J_9 with $J^{PC}=0^{++}$,

$$\begin{aligned}
\rho_9^{pert}(s) &= \frac{1}{128\pi^6}\int_{\alpha_{\min}}^{\alpha_{\max}} d\alpha \int_{\beta_{\min}}^{\beta_{\max}} d\beta \frac{(1-\alpha-\beta)^2[m_c^2(\alpha+\beta)-3\alpha\beta s][(\alpha+\beta)m_c^2-\alpha\beta s]^3}{\alpha^3\beta^3},\\
\rho_9^{\langle\bar{q}q\rangle}(s) &= \frac{m_c\langle\bar{q}q\rangle}{4\pi^4}\int_{\alpha_{\min}}^{\alpha_{\max}} d\alpha \int_{\beta_{\min}}^{\beta_{\max}} d\beta \frac{(1-\alpha-\beta)[(\alpha+\beta)m_c^2-\alpha\beta s][m_c^2(\alpha+\beta)-2\alpha\beta s]}{\alpha^2\beta},\\
\rho_9^{\langle GG\rangle}(s) &= \frac{\langle g_s^2 GG\rangle}{128\pi^6}\int_{\alpha_{\min}}^{\alpha_{\max}} d\alpha \int_{\beta_{\min}}^{\beta_{\max}} d\beta \left\{\frac{m_c^2(1-\alpha-\beta)^2[2m_c^2(\alpha+\beta)-3\alpha\beta s]}{3\beta^3}\right.\\
&\quad \left.+\frac{[m_c^2(\alpha+\beta)-2\alpha\beta s][(\alpha+\beta)m_c^2-\alpha\beta s]}{8}\left[\frac{(1-\alpha-\beta)^2}{2\alpha^2\beta^2}+\frac{(2-2\alpha-\beta)}{\alpha\beta^2}\right]\right\},\\
\rho_9^{\langle\bar{q}Gq\rangle}(s) &= \frac{m_c\langle\bar{q}g_s\sigma\cdot Gq\rangle}{64\pi^4}\int_{\alpha_{\min}}^{\alpha_{\max}} d\alpha \int_{\beta_{\min}}^{\beta_{\max}} d\beta \frac{(1-5\beta)[2m_c^2(\alpha+\beta)-3\alpha\beta s]}{\alpha\beta},\\
\rho_9^{\langle\bar{q}q\rangle^2}(s) &= \frac{m_c^2\langle\bar{q}q\rangle^2}{3\pi^2}\sqrt{1-4m_c^2/s},\\
\rho_9^{\langle\bar{q}q\rangle\langle\bar{q}Gq\rangle}(s) &= \frac{m_c^2\langle\bar{q}q\rangle\langle\bar{q}g_s\sigma\cdot Gq\rangle}{24\pi^2}\int_0^1 d\alpha\left\{\frac{4m_c^2}{\alpha^2}\delta'(s-\tilde{m}_c^2)-\frac{1}{\alpha}\delta(s-\tilde{m}_c^2)\right\}.
\end{aligned} \tag{A11}$$

For the current J_{10} with $J^{PC}=0^{++}$,

$$\begin{aligned}
\rho_{10}^{pert}(s) &= \frac{3}{64\pi^6}\int_{\alpha_{\min}}^{\alpha_{\max}} d\alpha \int_{\beta_{\min}}^{\beta_{\max}} d\beta \frac{(1-\alpha-\beta)^2[m_c^2(\alpha+\beta)-3\alpha\beta s][(\alpha+\beta)m_c^2-\alpha\beta s]^3}{\alpha^3\beta^3},\\
\rho_{10}^{\langle\bar{q}q\rangle}(s) &= \rho_{10}^{\langle\bar{q}Gq\rangle}(s)=0,\\
\rho_{10}^{\langle GG\rangle}(s) &= \frac{\langle g_s^2GG\rangle}{64\pi^6}\int_{\alpha_{\min}}^{\alpha_{\max}} d\alpha \int_{\beta_{\min}}^{\beta_{\max}} d\beta\left\{\frac{m_c^2(1-\alpha-\beta)^2[2m_c^2(\alpha+\beta)-3\alpha\beta s]}{\beta^3}\right.\\
&\quad\left.+\frac{[m_c^2(\alpha+\beta)-2\alpha\beta s][(\alpha+\beta)m_c^2-\alpha\beta s]}{2}\left[\frac{(1-\alpha-\beta)^2}{2\alpha^2\beta^2}+\frac{1}{\alpha\beta}\right]\right\},\\
\rho_{10}^{\langle\bar{q}q\rangle^2}(s) &= \frac{2m_c^2\langle\bar{q}q\rangle^2}{\pi^2}\sqrt{1-4m_c^2/s},\\
\rho_{10}^{\langle\bar{q}q\rangle\langle\bar{q}Gq\rangle}(s) &= \frac{m_c^2\langle\bar{q}q\rangle\langle\bar{q}g_s\sigma\cdot Gq\rangle}{\pi^2}\int_0^1 d\alpha\frac{m_c^2}{\alpha^2}\delta'(s-\tilde{m}_c^2).
\end{aligned}\tag{A12}$$

For the mixed current J^m with $J^{PC}=0^{++}$,

$$\begin{aligned}
\rho_m^{\rm pert}(s) &= \rho_m^{\langle\bar{q}q\rangle}(s)=\rho_m^{\langle\bar{q}q\rangle^2}(s)=0,\\
\rho_{10}^{\langle GG\rangle}(s) &= -\frac{3m_c^2\langle g_s^2GG\rangle}{1024\pi^6}\int_{\alpha_{\min}}^{\alpha_{\max}} d\alpha \int_{\beta_{\min}}^{\beta_{\max}} d\beta[(\alpha+\beta)m_c^2-\alpha\beta s]\left[\frac{(1-\alpha-\beta)}{\alpha\beta^2}+\frac{(1-\alpha-\beta)^2}{4\alpha^2\beta^2}+\frac{1}{2\alpha\beta}\right],\\
\rho_m^{\langle\bar{q}Gq\rangle}(s) &= -\frac{3m_c\langle\bar{q}g_s\sigma\cdot Gq\rangle}{128\pi^4}\int_{\alpha_{\min}}^{\alpha_{\max}} d\alpha \int_{\beta_{\min}}^{\beta_{\max}} d\beta\frac{(1-\beta)[2m_c^2(\alpha+\beta)-3\alpha\beta s]}{\alpha^2}\\
\rho_m^{\langle\bar{q}q\rangle\langle\bar{q}Gq\rangle}(s) &= \frac{\langle\bar{q}q\rangle\langle\bar{q}g_s\sigma\cdot Gq\rangle}{32\pi^2}\int_0^1 d\alpha\left\{\frac{m_c^2}{\alpha}\delta(s-\tilde{m}_c^2)+2\alpha\right\}.
\end{aligned}\tag{A13}$$

For the current $J_{11\mu\nu}$ with $J^{PC}=2^{++}$,

$$\begin{aligned}
\rho_{11}^{\rm pert}(s) &= \frac{1}{384\pi^6}\int_{\alpha_{\min}}^{\alpha_{\max}} d\alpha \int_{\beta_{\min}}^{\beta_{\max}} d\beta\left\{\frac{(1-\alpha-\beta)^3[m_c^2(\alpha+\beta)-5\alpha\beta s][3m_c^2(\alpha+\beta)-17\alpha\beta s][(\alpha+\beta)m_c^2-\alpha\beta s]^2}{2\alpha^3\beta^3}\right.\\
&\quad\left.-(1-\alpha-\beta)^2[(\alpha+\beta)m_c^2-\alpha\beta s]^3\left[\frac{13(1-\alpha-\beta)s}{\alpha^2\beta^2}-\frac{17m_c^2(\alpha+\beta)-81\alpha\beta s}{2\alpha^3\beta^3}\right]\right\},\\
\rho_{11}^{\langle\bar{q}q\rangle}(s) &= -\frac{5m_c\langle\bar{q}q\rangle}{2\pi^4}\int_{\alpha_{\min}}^{\alpha_{\max}} d\alpha \int_{\beta_{\min}}^{\beta_{\max}} d\beta\frac{(1-\alpha-\beta)[(\alpha+\beta)m_c^2-\alpha\beta s][m_c^2(\alpha+\beta)-3\alpha\beta s]}{\alpha^2\beta},\\
\rho_{11}^{\langle GG\rangle}(s) &= \frac{\langle g_s^2GG\rangle}{384\pi^6}\int_{\alpha_{\min}}^{\alpha_{\max}} d\alpha \int_{\beta_{\min}}^{\beta_{\max}} d\beta\left\{\frac{m_c^2(1-\alpha-\beta)^3[3m_c^2(\alpha+\beta)-16\alpha\beta s]}{3\alpha^3}\right.\\
&\quad+\frac{m_c^2(1-\alpha-\beta)^2[17m_c^2(\alpha+\beta)-33\alpha\beta s]}{3\alpha^3}-\frac{5[m_c^2(\alpha+\beta)-3\alpha\beta s][(\alpha+\beta)m_c^2-\alpha\beta s]}{4\alpha\beta}\\
&\quad\left.-\frac{5(1-\alpha-\beta)^2[5m_c^2(\alpha+\beta)-13\alpha\beta s][(\alpha+\beta)m_c^2-\alpha\beta s]}{48\alpha^2\beta^2}\right.
\end{aligned}$$

$$
\begin{aligned}
&- \frac{(1-\alpha-\beta)[29m_c^2(\alpha+\beta)-88\alpha\beta s][(\alpha+\beta)m_c^2-\alpha\beta s]}{3\alpha^2\beta} \\
&- \frac{5(1-\alpha-\beta)^3}{144\alpha^2\beta^2}[4(\alpha\beta s)^2-18\alpha\beta s[(\alpha+\beta)m_c^2-\alpha\beta s](s)+3[(\alpha+\beta)m_c^2-\alpha\beta s]^2] \\
&+ \frac{(1-\alpha-\beta)^2}{12\alpha^2\beta}[28(\alpha\beta s)^2-78\alpha\beta s[(\alpha+\beta)m_c^2-\alpha\beta s](s)+9[(\alpha+\beta)m_c^2-\alpha\beta s]^2]\Bigg\} \\
&+ \frac{7m_c^6\langle g_s^2GG\rangle}{1728\pi^6}\int_{\alpha_{\min}}^{\alpha_{\max}} d\alpha \frac{s^2(1-\alpha)[m_c^2-\alpha(1-\alpha)s]^3}{[m_c^2-(1-\alpha)s]^6}, \\
\rho_{11}^{\langle\bar{q}Gq\rangle}(s) &= \frac{5m_c\langle\bar{q}g_s\sigma\cdot Gq\rangle}{48\pi^4}\int_{\alpha_{\min}}^{\alpha_{\max}} d\alpha\int_{\beta_{\min}}^{\beta_{\max}} d\beta\frac{(1+12\alpha-\beta)[m_c^2(\alpha+\beta)-2\alpha\beta s]}{\alpha\beta}, \\
\rho_{11}^{\langle\bar{q}q\rangle^2}(s) &= \frac{10m_c^2\langle\bar{q}q\rangle^2}{3\pi^2}\sqrt{1-4m_c^2/s}, \\
\rho_{11}^{\langle\bar{q}q\rangle\langle\bar{q}Gq\rangle}(s) &= \frac{5m_c^2\langle\bar{q}q\rangle\langle\bar{q}g_s\sigma\cdot Gq\rangle}{36\pi^2}\int_0^1 d\alpha\left\{\frac{12m_c^2}{\alpha^2}\delta'(s-\tilde{m}_c^2)+\frac{1}{\alpha}\delta(s-\tilde{m}_c^2)\right\}.
\end{aligned}
\tag{A14}
$$

For the current $J_{12\mu\nu}$ with $J^{PC}=2^{++}$,

$$
\begin{aligned}
\rho_{12}^{\text{pert}}(s) &= \frac{1}{384\pi^6}\int_{\alpha_{\min}}^{\alpha_{\max}} d\alpha\int_{\beta_{\min}}^{\beta_{\max}} d\beta\Bigg\{\frac{(1-\alpha-\beta)^3[m_c^2(\alpha+\beta)-5\alpha\beta s][3m_c^2(\alpha+\beta)-17\alpha\beta s][(\alpha+\beta)m_c^2-\alpha\beta s]^2}{2\alpha^3\beta^3} \\
&\quad -(1-\alpha-\beta)^2[(\alpha+\beta)m_c^2-\alpha\beta s]^3\left[\frac{13(1-\alpha-\beta)s}{\alpha^2\beta^2}-\frac{17m_c^2(\alpha+\beta)-81\alpha\beta s}{2\alpha^3\beta^3}\right]\Bigg\}, \\
\rho_{12}^{\langle\bar{q}q\rangle}(s) &= \frac{5m_c\langle\bar{q}q\rangle}{2\pi^4}\int_{\alpha_{\min}}^{\alpha_{\max}} d\alpha\int_{\beta_{\min}}^{\beta_{\max}} d\beta\frac{(1-\alpha-\beta)[(\alpha+\beta)m_c^2-\alpha\beta s][m_c^2(\alpha+\beta)-3\alpha\beta s]}{\alpha^2\beta}, \\
\rho_{12}^{\langle GG\rangle}(s) &= \frac{\langle g_s^2GG\rangle}{384\pi^6}\int_{\alpha_{\min}}^{\alpha_{\max}} d\alpha\int_{\beta_{\min}}^{\beta_{\max}} d\beta\Bigg\{\frac{m_c^2(1-\alpha-\beta)^3[3m_c^2(\alpha+\beta)-16\alpha\beta s]}{3\alpha^3} \\
&\quad +\frac{m_c^2(1-\alpha-\beta)^2[17m_c^2(\alpha+\beta)-33\alpha\beta s]}{3\alpha^3}-\frac{5[m_c^2(\alpha+\beta)-3\alpha\beta s][(\alpha+\beta)m_c^2-\alpha\beta s]}{4\alpha\beta} \\
&\quad -\frac{5(1-\alpha-\beta)^2[5m_c^2(\alpha+\beta)-13\alpha\beta s][(\alpha+\beta)m_c^2-\alpha\beta s]}{48\alpha^2\beta^2} \\
&\quad -\frac{(1-\alpha-\beta)[29m_c^2(\alpha+\beta)-88\alpha\beta s][(\alpha+\beta)m_c^2-\alpha\beta s]}{3\alpha^2\beta} \\
&\quad -\frac{5(1-\alpha-\beta)^3}{144\alpha^2\beta^2}[4(\alpha\beta s)^2-18\alpha\beta s[(\alpha+\beta)m_c^2-\alpha\beta s](s)+3[(\alpha+\beta)m_c^2-\alpha\beta s]^2] \\
&\quad +\frac{(1-\alpha-\beta)^2}{12\alpha^2\beta}[28(\alpha\beta s)^2-78\alpha\beta s[(\alpha+\beta)m_c^2-\alpha\beta s](s)+9[(\alpha+\beta)m_c^2-\alpha\beta s]^2]\Bigg\} \\
&\quad +\frac{7m_c^6\langle g_s^2GG\rangle}{1728\pi^6}\int_{\alpha_{\min}}^{\alpha_{\max}} d\alpha\frac{s^2(1-\alpha)[m_c^2-\alpha(1-\alpha)s]^3}{[m_c^2-(1-\alpha)s]^6}, \\
\rho_{12}^{\langle\bar{q}Gq\rangle}(s) &= -\frac{5m_c\langle\bar{q}g_s\sigma\cdot Gq\rangle}{48\pi^4}\int_{\alpha_{\min}}^{\alpha_{\max}} d\alpha\int_{\beta_{\min}}^{\beta_{\max}} d\beta\frac{(1+12\alpha-\beta)[m_c^2(\alpha+\beta)-2\alpha\beta s]}{\alpha\beta}, \\
\rho_{12}^{\langle\bar{q}q\rangle^2}(s) &= \frac{10m_c^2\langle\bar{q}q\rangle^2}{3\pi^2}\sqrt{1-4m_c^2/s}, \\
\rho_{12}^{\langle\bar{q}q\rangle\langle\bar{q}Gq\rangle}(s) &= \frac{5m_c^2\langle\bar{q}q\rangle\langle\bar{q}g_s\sigma\cdot Gq\rangle}{36\pi^2}\int_0^1 d\alpha\left\{\frac{12m_c^2}{\alpha^2}\delta'(s-\tilde{m}_c^2)+\frac{1}{\alpha}\delta(s-\tilde{m}_c^2)\right\}.
\end{aligned}
\tag{A15}
$$

For the current $J_{13\mu\nu}$ with $J^{PC}=2^{++}$,

$$\begin{aligned}
\rho_{13}^{\rm pert}(s) &= \frac{1}{192\pi^6}\int_{\alpha_{\rm min}}^{\alpha_{\rm max}} d\alpha \int_{\beta_{\rm min}}^{\beta_{\rm max}} d\beta \Bigg\{ \frac{(1-\alpha-\beta)^3[m_c^2(\alpha+\beta)-5\alpha\beta s][3m_c^2(\alpha+\beta)-17\alpha\beta s][(\alpha+\beta)m_c^2-\alpha\beta s]^2}{2\alpha^3\beta^3} \\
&\quad -(1-\alpha-\beta)^2[(\alpha+\beta)m_c^2-\alpha\beta s]^3\left[\frac{13(1-\alpha-\beta)s}{\alpha^2\beta^2}-\frac{17m_c^2(\alpha+\beta)-81\alpha\beta s}{2\alpha^3\beta^3}\right]\Bigg\}, \\
\rho_{13}^{\langle\bar{q}q\rangle}(s) &= -\frac{5m_c\langle\bar{q}q\rangle}{\pi^4}\int_{\alpha_{\rm min}}^{\alpha_{\rm max}} d\alpha \int_{\beta_{\rm min}}^{\beta_{\rm max}} d\beta \frac{(1-\alpha-\beta)[(\alpha+\beta)m_c^2-\alpha\beta s][m_c^2(\alpha+\beta)-3\alpha\beta s]}{\alpha^2\beta}, \\
\rho_{13}^{\langle GG\rangle}(s) &= \frac{\langle g_s^2GG\rangle}{576\pi^6}\int_{\alpha_{\rm min}}^{\alpha_{\rm max}} d\alpha \int_{\beta_{\rm min}}^{\beta_{\rm max}} d\beta \Bigg\{ \frac{m_c^2(1-\alpha-\beta)^3[3m_c^2(\alpha+\beta)-16\alpha\beta s]}{\alpha^3} \\
&\quad +\frac{m_c^2(1-\alpha-\beta)^2[17m_c^2(\alpha+\beta)-33\alpha\beta s]}{\alpha^3}-\frac{25[m_c^2(\alpha+\beta)-2\alpha\beta s][(\alpha+\beta)m_c^2-\alpha\beta s]}{4\alpha\beta} \\
&\quad -\frac{25(1-\alpha-\beta)^2[5m_c^2(\alpha+\beta)-13\alpha\beta s][(\alpha+\beta)m_c^2-\alpha\beta s]}{32\alpha^2\beta^2} \\
&\quad -\frac{(1-\alpha-\beta)[16m_c^2(\alpha+\beta)-47\alpha\beta s][(\alpha+\beta)m_c^2-\alpha\beta s]}{2\alpha^2\beta} \\
&\quad -\frac{25(1-\alpha-\beta)^3}{96\alpha^2\beta^2}[4(\alpha\beta s)^2-18\alpha\beta s[(\alpha+\beta)m_c^2-\alpha\beta s]+3[(\alpha+\beta)m_c^2-\alpha\beta s]^2] \\
&\quad -\frac{(1-\alpha-\beta)^2}{8\alpha^2\beta}[28(\alpha\beta s)^2-78\alpha\beta s[(\alpha+\beta)m_c^2-\alpha\beta s]+9[(\alpha+\beta)m_c^2-\alpha\beta s]^2]\Bigg\} \\
&\quad +\frac{7m_c^6\langle g_s^2GG\rangle}{864\pi^6}\int_{\alpha_{\rm min}}^{\alpha_{\rm max}} d\alpha \frac{s^2(1-\alpha)[m_c^2-\alpha(1-\alpha)s]^3}{[m_c^2-(1-\alpha)s]^6}, \\
\rho_{13}^{\langle\bar{q}Gq\rangle}(s) &= \frac{5m_c\langle\bar{q}g_s\sigma\cdot Gq\rangle}{48\pi^4}\int_{\alpha_{\rm min}}^{\alpha_{\rm max}} d\alpha \int_{\beta_{\rm min}}^{\beta_{\rm max}} d\beta \frac{(5+24\alpha-5\beta)[m_c^2(\alpha+\beta)-2\alpha\beta s]}{\alpha\beta}, \\
\rho_{13}^{\langle\bar{q}q\rangle^2}(s) &= \frac{20m_c^2\langle\bar{q}q\rangle^2}{3\pi^2}\sqrt{1-4m_c^2/s}, \\
\rho_{13}^{\langle\bar{q}q\rangle\langle\bar{q}Gq\rangle}(s) &= \frac{5m_c^2\langle\bar{q}q\rangle\langle\bar{q}g_s\sigma\cdot Gq\rangle}{36\pi^2}\int_0^1 d\alpha\left\{\frac{24m_c^2}{\alpha^2}\delta'(s-\tilde{m}_c^2)+\frac{5}{\alpha}\delta(s-\tilde{m}_c^2)\right\}.
\end{aligned} \tag{A16}$$

For the current $J_{14\mu\nu}$ with $J^{PC}=2^{++}$,

$$\begin{aligned}
\rho_{14}^{pert}(s) &= \frac{1}{192\pi^6}\int_{\alpha_{\rm min}}^{\alpha_{\rm max}} d\alpha \int_{\beta_{\rm min}}^{\beta_{\rm max}} d\beta \Bigg\{ \frac{(1-\alpha-\beta)^3[m_c^2(\alpha+\beta)-5\alpha\beta s][3m_c^2(\alpha+\beta)-17\alpha\beta s][(\alpha+\beta)m_c^2-\alpha\beta s]^2}{2\alpha^3\beta^3} \\
&\quad -(1-\alpha-\beta)^2[(\alpha+\beta)m_c^2-\alpha\beta s]^3\left[\frac{13(1-\alpha-\beta)s}{\alpha^2\beta^2}-\frac{17m_c^2(\alpha+\beta)-81\alpha\beta s}{2\alpha^3\beta^3}\right]\Bigg\}, \\
\rho_{14}^{\langle\bar{q}q\rangle}(s) &= \frac{5m_c\langle\bar{q}q\rangle}{\pi^4}\int_{\alpha_{\rm min}}^{\alpha_{\rm max}} d\alpha \int_{\beta_{\rm min}}^{\beta_{\rm max}} d\beta \frac{(1-\alpha-\beta)[(\alpha+\beta)m_c^2-\alpha\beta s][m_c^2(\alpha+\beta)-3\alpha\beta s]}{\alpha^2\beta}, \\
\rho_{14}^{\langle GG\rangle}(s) &= \frac{\langle g_s^2GG\rangle}{576\pi^6}\int_{\alpha_{\rm min}}^{\alpha_{\rm max}} d\alpha \int_{\beta_{\rm min}}^{\beta_{\rm max}} d\beta \Bigg\{ \frac{m_c^2(1-\alpha-\beta)^3[3m_c^2(\alpha+\beta)-16\alpha\beta s]}{\alpha^3}
\end{aligned}$$

$$
\begin{aligned}
&+\frac{m_c^2(1-\alpha-\beta)^2[17m_c^2(\alpha+\beta)-33\alpha\beta s]}{\alpha^3}-\frac{25[m_c^2(\alpha+\beta)-2\alpha\beta s][(\alpha+\beta)m_c^2-\alpha\beta s]}{4\alpha\beta}\\
&-\frac{25(1-\alpha-\beta)^2[5m_c^2(\alpha+\beta)-13\alpha\beta s][(\alpha+\beta)m_c^2-\alpha\beta s]}{32\alpha^2\beta^2}\\
&-\frac{(1-\alpha-\beta)[16m_c^2(\alpha+\beta)-47\alpha\beta s][(\alpha+\beta)m_c^2-\alpha\beta s]}{2\alpha^2\beta}\\
&-\frac{25(1-\alpha-\beta)^3}{96\alpha^2\beta^2}[4(\alpha\beta s)^2-18\alpha\beta s[(\alpha+\beta)m_c^2-\alpha\beta s]+3[(\alpha+\beta)m_c^2-\alpha\beta s]^2]\\
&-\frac{(1-\alpha-\beta)^2}{8\alpha^2\beta}[28(\alpha\beta s)^2-78\alpha\beta s[(\alpha+\beta)m_c^2-\alpha\beta s]+9[(\alpha+\beta)m_c^2-\alpha\beta s]^2]\Big\}\\
&+\frac{7m_c^6\langle g_s^2GG\rangle}{864\pi^6}\int_{\alpha_{\min}}^{\alpha_{\max}}d\alpha\frac{s^2(1-\alpha)[m_c^2-\alpha(1-\alpha)s]^3}{[m_c^2-(1-\alpha)s]^6},\\
\rho_{14}^{\langle\bar{q}Gq\rangle}(s)&=-\frac{5m_c\langle\bar{q}g_s\sigma\cdot Gq\rangle}{48\pi^4}\int_{\alpha_{\min}}^{\alpha_{\max}}d\alpha\int_{\beta_{\min}}^{\beta_{\max}}d\beta\frac{(5+24\alpha-5\beta)[m_c^2(\alpha+\beta)-2\alpha\beta s]}{\alpha\beta},\\
\rho_{14}^{\langle\bar{q}q\rangle^2}(s)&=\frac{20m_c^2\langle\bar{q}q\rangle^2}{3\pi^2}\sqrt{1-4m_c^2/s},\\
\rho_{14}^{\langle\bar{q}q\rangle\langle\bar{q}Gq\rangle}(s)&=\frac{5m_c^2\langle\bar{q}q\rangle\langle\bar{q}g_s\sigma\cdot Gq\rangle}{36\pi^2}\int_0^1d\alpha\left\{\frac{24m_c^2}{\alpha^2}\delta'(s-\tilde{m}_c^2)+\frac{5}{\alpha}\delta(s-\tilde{m}_c^2)\right\}.
\end{aligned}
\tag{A17}
$$

[1] S. Uehara *et al.* (Belle Collaboration), Phys. Rev. Lett. **96**, 082003 (2006).
[2] S. Uehara *et al.* (Belle Collaboration), Phys. Rev. Lett. **104**, 092001 (2010).
[3] C. P. Shen *et al.* (Belle Collaboration), Phys. Rev. Lett. **104**, 112004 (2010).
[4] P. Pakhlov *et al.* (Belle Collaboration), Phys. Rev. Lett. **100**, 202001 (2008).
[5] K. Chilikin *et al.* (Belle Collaboration), Phys. Rev. D **95**, 112003 (2017).
[6] S. Godfrey and N. Isgur, Phys. Rev. D **32**, 189 (1985).
[7] T. Barnes, S. Godfrey, and E. S. Swanson, Phys. Rev. D **72**, 054026 (2005).
[8] C. Patrignani *et al.* (Particle Data Group Collaboration), Chin. Phys. C **40**, 100001 (2016).
[9] X. Liu, Z.-G. Luo, and Z.-F. Sun, Phys. Rev. Lett. **104**, 122001 (2010).
[10] Y. Jiang, G.-L. Wang, T. Wang, and W.-L. Ju, Int. J. Mod. Phys. A **28**, 1350145 (2013).
[11] F.-K. Guo, C. Hanhart, G. Li, U.-G. Meissner, and Q. Zhao, Phys. Rev. D **83**, 034013 (2011).
[12] Z.-Y. Zhou and Z. Xiao, Phys. Rev. D **96**, 054031 (2017).
[13] R. F. Lebed and A. D. Polosa, Phys. Rev. D **93**, 094024 (2016).
[14] Z.-G. Wang, Eur. Phys. J. C **77**, 78 (2017).
[15] R. M. Albuquerque, M. E. Bracco, and M. Nielsen, Phys. Lett. B **678**, 186 (2009).
[16] J. R. Zhang and M. Q. Huang, J. Phys. G **37**, 025005 (2010).
[17] Z. G. Wang, Eur. Phys. J. C **63**, 115 (2009).
[18] Z. G. Wang, Z. C. Liu, and X. H. Zhang, Eur. Phys. J. C **64**, 373 (2009).
[19] H. X. Chen, E. L. Cui, W. Chen, X. Liu, and S. L. Zhu, Eur. Phys. J. C **77**, 160 (2017).
[20] Z.-G. Wang, Eur. Phys. J. A **53**, 192 (2017).
[21] G. L. Yu, Z. G. Wang, and Z. Y. Li, arXiv:1704.06763.
[22] K.-T. Chao, Phys. Lett. B **661**, 348 (2008).
[23] B.-Q. Li and K.-T. Chao, Phys. Rev. D **79**, 094004 (2009).
[24] L.-P. He, D.-Y. Chen, X. Liu, and T. Matsuki, Eur. Phys. J. C **74**, 3208 (2014).
[25] R. Molina and E. Oset, Phys. Rev. D **80**, 114013 (2009).
[26] W. H. Liang, J. J. Xie, E. Oset, R. Molina, and M. Doring, Eur. Phys. J. A **51**, 58 (2015).
[27] Z. H. Guo and J. A. Oller, Phys. Rev. D **93**, 096001 (2016).
[28] L. R. Dai, J. J. Xie, and E. Oset, Eur. Phys. J. C **76**, 121 (2016).
[29] H.-X. Chen, W. Chen, X. Liu, and S.-L. Zhu, Phys. Rep. **639**, 1 (2016).
[30] A. Esposito, A. Pilloni, and A. D. Polosa, Phys. Rep. **668**, 1 (2017).
[31] R. F. Lebed, R. E. Mitchell, and E. S. Swanson, Prog. Part. Nucl. Phys. **93**, 143 (2017).
[32] F.-K. Guo, C. Hanhart, U.-G. Meiner, Q. Wang, Q. Zhao, and B.-S. Zou, arXiv:1705.00141.
[33] H. X. Chen, W. Chen, X. Liu, Y. R. Liu, and S. L. Zhu, Rep. Prog. Phys. **80**, 076201 (2017).

[34] H. X. Chen, A. Hosaka, and S. L. Zhu, Phys. Rev. D **76**, 094025 (2007).
[35] M.-L. Du, W. Chen, X.-L. Chen, and S.-L. Zhu, Phys. Rev. D **87**, 014003 (2013).
[36] W. Chen, T. Steele, and S.-L. Zhu, Phys. Rev. D **89**, 054037 (2014).
[37] W. Chen and S.-L. Zhu, Phys. Rev. D **83**, 034010 (2011).
[38] W. Chen and S.-L. Zhu, Phys. Rev. D **81**, 105018 (2010).
[39] H.-X. Chen, Q. Mao, W. Chen, A. Hosaka, X. Liu, and S.-L. Zhu, Phys. Rev. D **95**, 094008 (2017).
[40] M. Eidemuller and M. Jamin, Phys. Lett. B **498**, 203 (2001).
[41] M. Jamin and A. Pich, Nucl. Phys. B, Proc. Suppl. **74**, 300 (1999).
[42] M. Jamin, J. A. Oller, and A. Pich, Eur. Phys. J. C **24**, 237 (2002).
[43] A. Khodjamirian, T. Mannel, N. Offen, and Y.-M. Wang, Phys. Rev. D **83**, 094031 (2011).
[44] T. Kojo, A. Hayashigaki, and D. Jido, Phys. Rev. C **74**, 045206 (2006).
[45] T. Kojo and D. Jido, Phys. Rev. D **78**, 114005 (2008).
[46] R. Jaffe, Phys. Rep. **409**, 1 (2005).